Application of Fluorescence Correlation Spectroscopy to the Measurement of Local Temperature in Solutions under Optical Trapping Condition

Syoji Ito,* Takashi Sugiyama, Naoki Toitani, Genki Katayama, and Hiroshi Miyasaka*

Division of Frontier Materials Science, Graduate School of Engineering Science and Center for Quantum Materials Science under Extreme Conditions, Osaka University, Toyonaka, Osaka 560-8531, Japan

Received: August 10, 2006; In Final Form: November 21, 2006

Fluorescence correlation spectroscopy (FCS) was applied to the quantitative evaluation of the local heating in small domains <1 μm in solutions under the laser trapping condition in the presence of a near-infrared (NIR) laser beam at 1064 nm. On the basis of the translational diffusion coefficient of fluorescent molecules obtained by FCS, the relationship between temperature rise and the incident NIR laser power, $\Delta T/\Delta P$, were determined to be 62 ± 6, 49 ± 7, and 23 ± 1 deg K/W in ethylene glycol, ethanol, and water, respectively, while no remarkable temperature increase was observed for deuterated water. The value of $\Delta T/\Delta P$ linearly increased as a function of α/λ (α is the extinction coefficient of solvent at the wavelength and λ is the thermal conductivity of the medium). The validity and the applicability of the present method for the measurement of the local temperature increase were discussed by comparing the present results with previous ones by other various methods.

Introduction

Since the pioneering work[1] of Ashkin in 1986, laser trapping (optical tweezers) has been used as a powerful microscopic manipulation tool in the fabrication and the elucidation of various small systems. In these years the target of this method has been downsized from micrometer-scaled objects to nanometer-sized systems, such as patterning of individual nanoparticles onto substrates in solution by using photochemical/photothermal reactions,[2−4] formation of polymer microparticles with characteristic internal structure by assembling polymer chains with the photon force,[5,6] force measurement of individual motor proteins in molecular cell biology,[7,8] and so on.

In the typical condition of the laser trapping, a continuous wave (CW) from a near-infrared (NIR) laser, such as a Nd^{3+}:YAG or a Nd^{3+}:YVO_4 system, is tightly focused into a spot close to its diffraction limit through a high numerical aperture (NA) microscope objective. This tight focusing exerts a photon force on a particle with refractive index higher than that of the surrounding medium, leading to the movement of the particle toward the area of higher optical field; as a result, the optical geometry realizes only one stable trapping point (potential minimum) at the focus.[1] To achieve stable trapping, the laser power of tens to hundreds of mW is introduced into the focus, resulting in a power intensity of $\sim$MW/cm^2 under the objective. This strong light field can easily induce temperature elevation around the focal point of the NIR beam even in water and other organic solvents with small absorption probability in the NIR region. Because physical properties, chemical reactivities, and biological activities are sensitively dependent on the temperature, the quantitative estimation under the trapping condition is indispensable for the rational interpretation and the application of the laser trapping.

* Corresponding authors. S.I.: e-mail sito@chem.es.osaka-u.ac.jp; phone +81-6-6850-6243, fax +81-6-6850-6244. H.M.: e-mail: miyasaka@chem.es.osaka-u.ac.jp; phone +81-6-6850-6241; fax +81-6-6850-6244.

Several investigations have been published on this temperature elevation by the trapping laser beam for various systems in water. Fischer et al. reported the temperature increase, ΔT, versus the incident power of a CW YAG laser at 1064 nm, ΔP, as $\Delta T/\Delta P \approx 5$ deg K/W by observing the thermal phase transition of a Langmuir monolayer at an air−water interface.[9] Tromberg et al.[10,11] reported the $\Delta T/\Delta P$ value of 10−14.5 deg K/W in liposomes and Chinese hamster ovary cells by using the phase transition of the lipid bilayers. Conia et al. estimated a short-time temperature elevation of $\sim$40 deg K/W induced by 985 nm laser irradiation for 250 ms using the interferometric technique.[12] Schmidt et al. reported an $\sim$8 deg K/W temperature increase by analysis of the thermal motion of a trapped microbead with submicrometer to several micrometer size.[13] For formulating the temperature elevation, Hell et al.[14] calculated an $\sim$19 deg K/W temperature rise under irradiation of 1050 nm laser light for 10 s.

Although these methods have contributed to the estimation of the local temperature increase, there exists almost one order of difference in $\Delta T/\Delta P$ depending on the systems and methods of estimation for the temperature increase. As already pointed out above, evaluation of the local temperature in the steady state under NIR laser irradiation is indispensable to the rational interpretation and the comprehensive application of the optical tweezers. To precisely and accurately determine the temperature in solvents under the optical trapping condition, we have applied fluorescence correlation spectroscopy (FCS) in the present work. One of the advantages of this method is that an extremely dilute concentration of probe molecules does not lead to the temperature increase via the absorption by the solutes and we can attribute the temperature rise to the absorption of the NIR laser light by solvents; change in the diffusive motion of the fluorescent dye molecules dependent on the temperature is directly detected and these data can provide the local temperature via the analysis. Hence the method enables us to measure temperature in solution with high spatial resolution less than 400 nm in the plane orthogonal to the optical axis. In the

10.1021/jp065156l CCC: $37.00 © 2007 American Chemical Society
Published on Web 02/09/2007

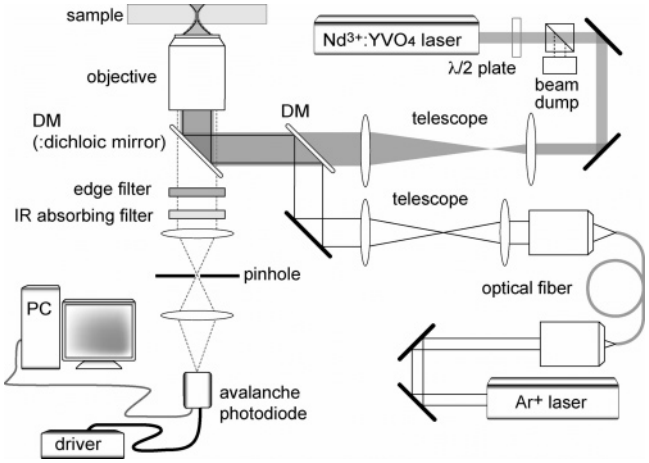

Figure 1. Schematic illustration of a laser trapping FCS system. The near-infrared beam from a Nd:YVO_4 laser (1064 nm) was expanded by 3 times and re-collimated by lenses of $f = 100$ and 300 mm, then was focused by a high NA objective (NA = 1.35, ×100) close to its diffraction limit. The power of the NIR laser beam was adjusted by using a half-wave plate and a polarizing beam splitter. The excitation laser light with 488 nm wavelength from a Ar^+ laser was focused in a similar manner without magnification; two lenses in the optical path were the same in focal length. The focusing points of these two laser beams were controlled by the pairs of lenses both in the focal plane and along the optical axis of the objective. Fluorescence from the confocal volume in the sample solution was detected by an avalanche photodiode; the sampling area was typically 350 nm in diameter in the focal plane.

following, we will present the experimental setup, principle of the measurement, and experimental results on the $\Delta T/\Delta P$ relationships. In addition, we will discuss these values in view of the extinction coefficient of the solvents at 1064 nm and the thermal conductivity of the solvents.

Samples and Experimental Setup

The setup for the FCS measurement at the optical trapping point is schematically illustrated in Figure 1. As an excitation light source for the FCS measurement, a CW Ar^+ laser (LGK7872M, LASOS lasertechnik GmbH) at 488 nm was coupled to a single mode optical fiber to isolate the laser device from an optical bench. This excitation laser light transmitted through the optical fiber was collimated with a pair of lenses, and then was focused by a microscope objective lens (UPlanApo 100X Oil Iris3, NA: 1.35, Olympus). The detection volume (confocal volume) of the FCS measurement was determined by a pinhole (typically 25 μm) attached to an optical microscope (IX70, Olympus). The emitted photons from dye molecules inside the confocal volume were detected with an avalanche photodiode (SPCM-AQR-14, Perkin-Elmer) connected with a counting board (M9003, Hamamatsu photonics K.K.). Scattered light from the sampling volume was blocked by an edge (long-pass) filter (Semrock, LP01-488RU) for the 488 nm light and an IR absorbing filter (Sigma Koki, HAF-50S-30H) for the 1064 nm light. The autocorrelation function of the fluorescent intensity was obtained by using FCS software (U9451, Hamamatsu photonics K.K.) that calculated the autocorrelation function from the integrated data of photons for ~3 s. In the present study, we accumulated the autocorrelation functions 20−30 times to obtain the data with high signal-to-noise (S/N) ratio.

A CW laser beam from a Nd:YVO_4 laser (J20-BF-106W, Spectra-Physics) was focused as NIR light at 1064 nm by the microscope objective lens in a similar manner. NIR laser power in solution through the objective was estimated by a reported method by Masuhara et al. in 1991.[15] Briefly, the NIR laser beam was focused by the microscope objective then re-collimated by the same type of objective. The gap between the two objectives was filled with immersion oil. The diameter of the incident laser beam to the objective was adjusted to the same size as the entrance port of the objective by a metal aperture. The fraction of the input power I_{in} and output power I_{out} was measured with a power meter, estimating the transmittance of the objective T_{obj} from the equation of $T_{obj}^2 = I_{out}/I_{in}$.

Rhodamine-6G (R6G; Nippon Kanko Shikiso) and Rhodamine-123 (R123; Acros Organics) were used as fluorescent probes without further purification. The solutions of water (Wako), D_2O (Cambridge Isotope Laboratories), ethanol (99.5%, Kshida), and ethylene glycol (99.5%, Wako) including these fluorescent molecules were injected into glass-bottom culture dishes (MatTek) for measurement. Through all measurements, both focusing points of the blue laser light and the NIR light were adjusted 30 μm above from the bottom of the culture dishes except for the measurement on the effect of the distance on the temperature elevation.

Principle of the Measurement

Fluorescence correlation spectroscopy provides the information on the molecular motion, translational diffusion coefficient, on the basis of the fluctuation of fluorescence intensity in the time domain. The autocorrelation function, $G(\tau)$, of this fluorescence fluctuation at the confocal volume is analytically derived by the following equation[16,17]

$$G(\tau) = 1 + \frac{1}{N}\left[1 + \frac{p}{1-p}\exp\left(-\frac{\tau}{\tau_T}\right)\right]\left(1 + \frac{\tau}{\tau_D}\right)^{-1}\left(1 + \frac{\tau}{w^2\tau_D}\right)^{-1/2} \quad (1)$$

where N is the average number of molecules in the confocal volume, V_{conf}, with cylindrical shape, p is the fraction of the contribution of triplet state, τ_T is triplet lifetime, and w is the structure parameter defined by $w = w_z/w_{xy}$. Here, w_z and w_{xy} are respectively the axial length and radial radii of the cylindrical confocal volume ($V_{conf} = 2\pi w_z w_{xy}^2$). τ_D is the diffusion time related to the translational diffusion coefficient, D, as represented by eq 2.

$$\tau_D = \frac{w_{xy}^2}{4D} \quad (2)$$

The analysis of the autocorrelation function on the basis of eq 1 provides the diffusion time, τ_D, which is related to the viscosity of the solution and the temperature. Under the condition that the translational diffusion coefficient, D, is represented by the Stokes−Einstein model (eq 3), the diffusion time, τ_D, obtained by the analysis of the autocorrelation curve is given by eq 4.

$$D = \frac{kT}{6\pi\eta(T)a} \quad (3)$$

$$\frac{\gamma}{\tau_D} = \frac{T}{\eta(T)} \qquad \left(\gamma = \frac{6\pi a w_{xy}^2}{4k}\right) \quad (4)$$

Here, k is Boltzmann's constant, T is the temperature (Kelvin), $\eta(T)$ is the viscosity of solution at temperature T, and a is the hydrodynamic radius of a probe molecule. Elimination of D between eqs 2 and 3 gives eq 4.

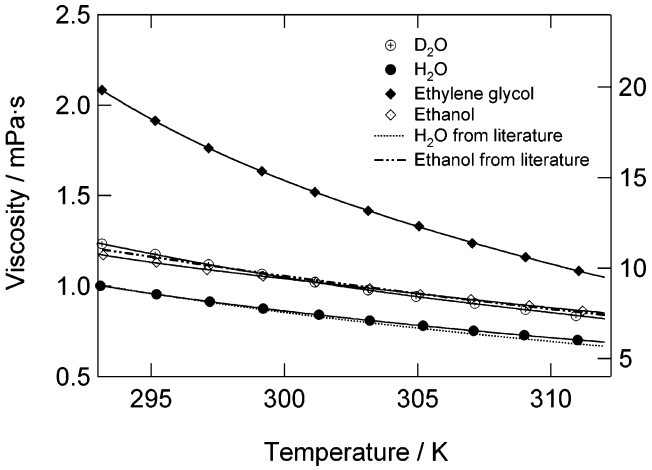

Figure 2. Viscosity−temperature dependence of solvents used in the present experiment. The value on the left axis is for H_2O, D_2O, and ethanol, and that on the right axis is for ethylene glycol.

The $\eta(T)$ value independently measured by a viscometer and the γ value obtained by the FCS measurement at a certain temperature (typically 21−22 °C) allow the estimation of T in eq 4 under the condition that the hydrodynamic diameter of the probe molecule is constant in the temperature range of this series of experiments. It should be noted that the present method determines the average temperature inside the sampling volume of the FCS measurement because FCS provides the average value of translational diffusion velocity over fluorescent molecules passing through the confocal area.

Experimental Results

The temperature dependence of the viscosity of solvents used in the present work was experimentally obtained by using an Ostwald viscometer as shown in Figure 2. Each value in the figure is averaged over five measurements. Error bars are not presented in the viscosity−temperature dependence because the measured viscosities exhibited quite high repeatability with an accuracy of less than 0.5%, which are hidden behind the makers in the figure. All data points were interpolated by using polynomial to estimate intermediate values. The values for water and ethanol obtained by the present measurement reproduced the values presented in ref 18 quite well as shown in Figure 2, indicating the present measurements provided reliable values of the viscosities in the temperature region examined here.

Extinction coefficients of solvents used in the present study were determined by measuring the transmittance of the NIR laser light at 1064 nm passing through a cylindrical vessel filled with the solvents with various volumes (optical path length). Figure 3 shows the transmittance of the NIR laser light as a function of the optical path length through the solvents. The transmittance of the NIR laser light decreased with an increase in the optical path length on the basis of Lambert−Beer's law. From the results in Figure 3, we obtained extinction coefficients of 14.5 m^{-1} (1.1×10^{-3} M^{-1} cm^{-1}) for water, 11.2 m^{-1} (2.8×10^{-3} M^{-1} cm^{-1}) for ethanol, and 19.9 m^{-1} (4.8×10^{-3} M^{-1} cm^{-1}) for ethylene glycol. The extinction coefficient of pure water obtained in the present measurement is almost the same as the values that were reported to be 14.2 and 12 m^{-1} at 1064 nm in refs 13 and 23, respectively. Although we could not find reference values for ethanol and ethylene glycol, the good agreement of the present extinction coefficient of water with the values in the previous report indicates the NIR laser irradiation induces only linear absorption by the solvent and the nonlinear process can be ignored. These extinction coefficients were used for the quantitative analysis of the temperature increase, as will be discussed later.

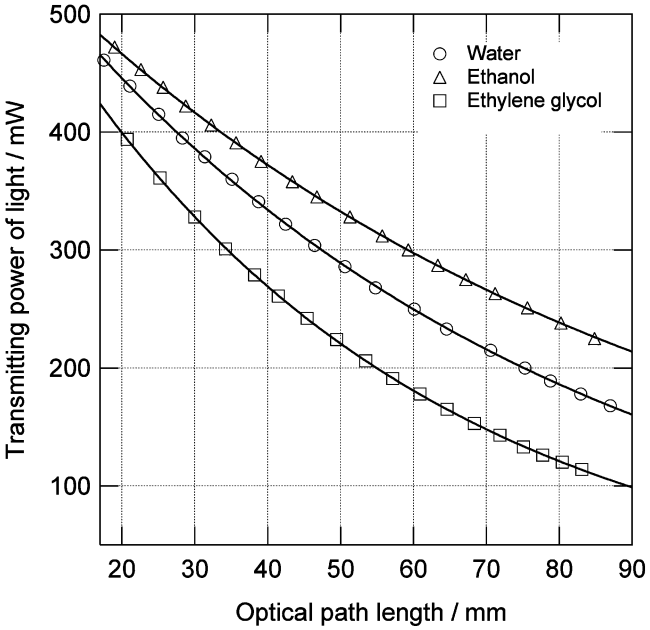

Figure 3. Transmitting power of the NIR laser light passing through the solvents used in the present work as a function of path length. The transmitting laser power decreases exponentially with an increase in the path length in accordance with Lambert−Beer's law.

Figure 4 shows fluorescence autocorrelation curves of R6G in ethylene glycol (a) and R123 in water (b) at 294.4 K. The solid line in each of the traces is the curve analyzed by the nonlinear least-squares method with eq 1 and the residual is plotted in the top of each trace, indicating that the experimental results were well reproduced by the calculated curve. Thanks to the high S/N ratio of the experimental data, the values of the five parameters in eq 1, i.e., N, τ_D, w, p, and τ_T, obtained through the analysis exhibited quite good repeatability within ±0.5% at several trials of the nonlinear least-squares method even though all the parameters were not fixed in the procedure. Also for other solutions of heavy water and ethanol, it was confirmed that the analysis based on eq 1 well reproduced the experimental results.

As already described, the lateral size of the volume element, w_{xy}, is related to the diffusion time, τ_D, and the diffusion coefficient, D, by eq 2. The lateral size of the volume element, w_{xy}, under the present experimental condition was determined to be 350 nm in diameter on the basis of the diffusion constants of R6G[19,20] (2.8×10^{-10} m^2/s) and R123[21] (3.0×10^{-10} m^2/s) in water as reference.

In Figure 5a, we exhibit the fluorescence autocorrelation curves of R6G in ethylene glycol in the presence of the incident NIR laser light, clearly indicating that the decay of the correlation curve becomes fast with an increase in the incident NIR laser power. A similar dependence on the NIR intensity was observed in the case of the aqueous solution of R123 as shown in Figure 5b.

Figure 6 shows the fluorescence correlation signals obtained for the R6G solution of ethylene glycol and the R123 solution of water under the irradiation of the NIR laser at 240 mW, together with the curves calculated by using eq 1 and the residuals. The correlation function curves under the NIR laser irradiation are well reproduced by eq 1, as was shown in Figure 4 without incident NIR laser light.

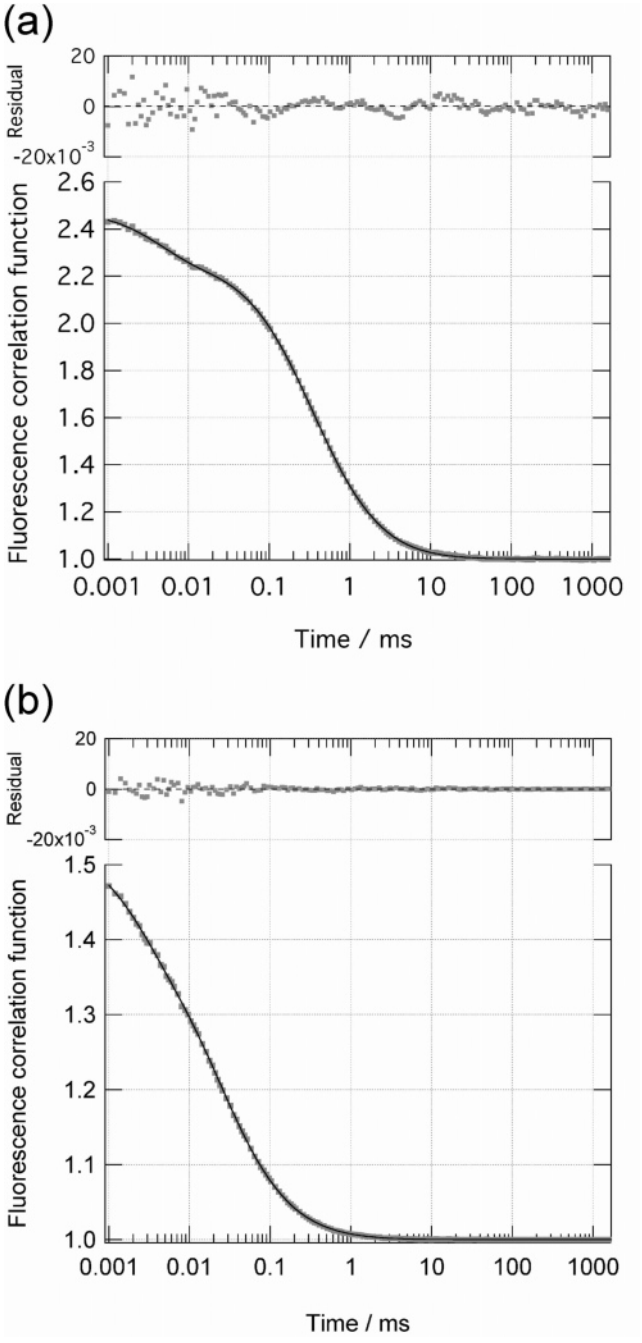

Figure 4. Typical fluorescence autocorrelation curves of the R6G in ethylene glycol (a) and R123 in water (b) without the NIR laser light, and their fitting curves based on eq 2 and residuals. Experimental data were plotted as gray dots and theoretical curves were drawn in a black solid line.

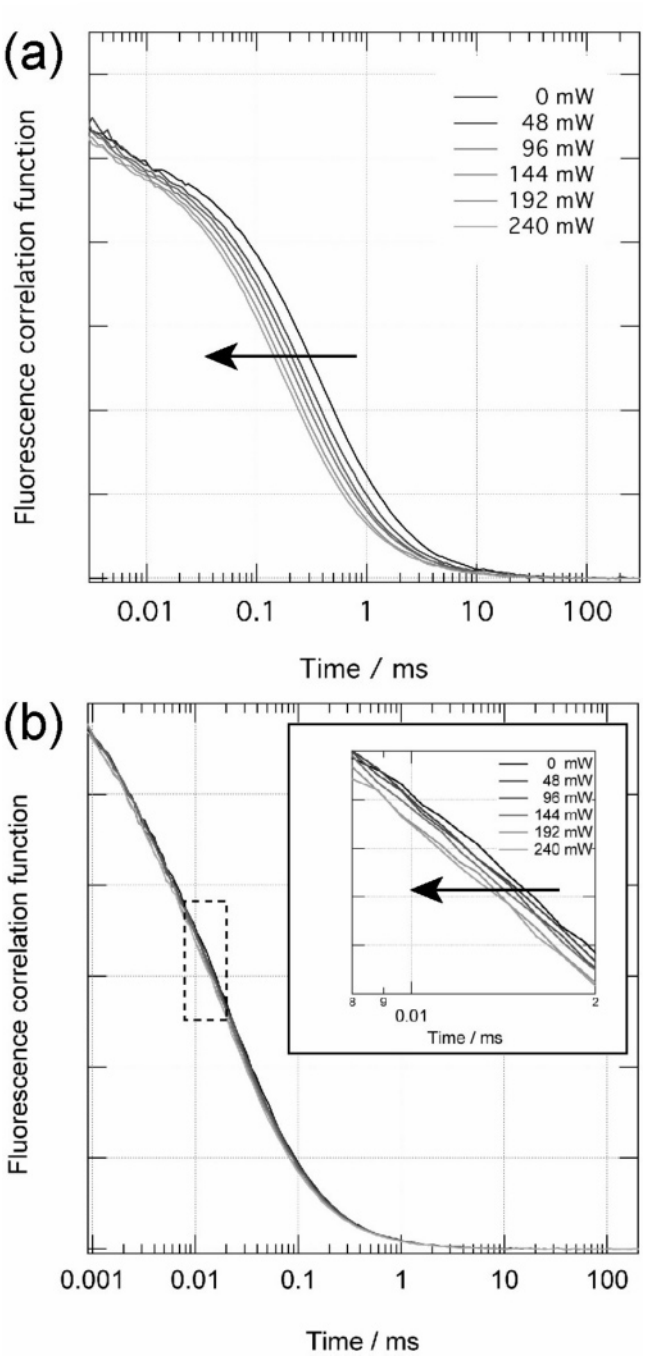

Figure 5. Dependence of the autocorrelation curve on the power of the incident NIR laser light. The fluorescence autocorrelation curves of R6G in ethylene glycol (a) and R123 in water (b) decay faster with increasing the NIR laser power. The inset of Figure 5b shows a magnified view of a part of the figure enclosed by a dotted rectangle.

On the change of the translational motion of the molecule, it is worth noting that the tight focusing of the NIR laser light results in the trapping of small particles. The optical force that the particle experiences is dependent on its size and the intensity of the incident laser, and a simple model using Rayleigh approximation[1] predicted that the optical force potential depth of the ~10 nm particle under the incident beam of several hundreds of mW was equal to the average energy of thermal motion at room temperature ($\sim 4.0 \times 10^{-21}$ J). That is, a particle size of at least 10−20 nm in diameter is necessary for effective optical trapping. Because the Rhodamine molecules are ~1 nm in size (estimated from its diffusion coefficient in water) and the optical force potential depth is proportional to the volume of the particle, the optical force for these molecules can be estimated to be $\leq 10^{-3}$ kT, indicating that the change of decay in the autocorrelation function under the NIR laser irradiation is attributed to the acceleration of the molecular motion by temperature elevation and this motion is not influenced by the optical force. Indeed, the diffusion time of the R6G was not influenced at all by the radiation pressure of the NIR laser light in deuterated water without significant absorption for the wavelength of the NIR region (data are summarized in Figure 7d). Summarizing the above results and discussion, we can conclude that an estimation of the local temperature in the sample solutions based on eq 4 can provide reliable values.

Figure 7 shows the temperature at the focal point of the NIR laser beam obtained by the analysis of the correlation curves

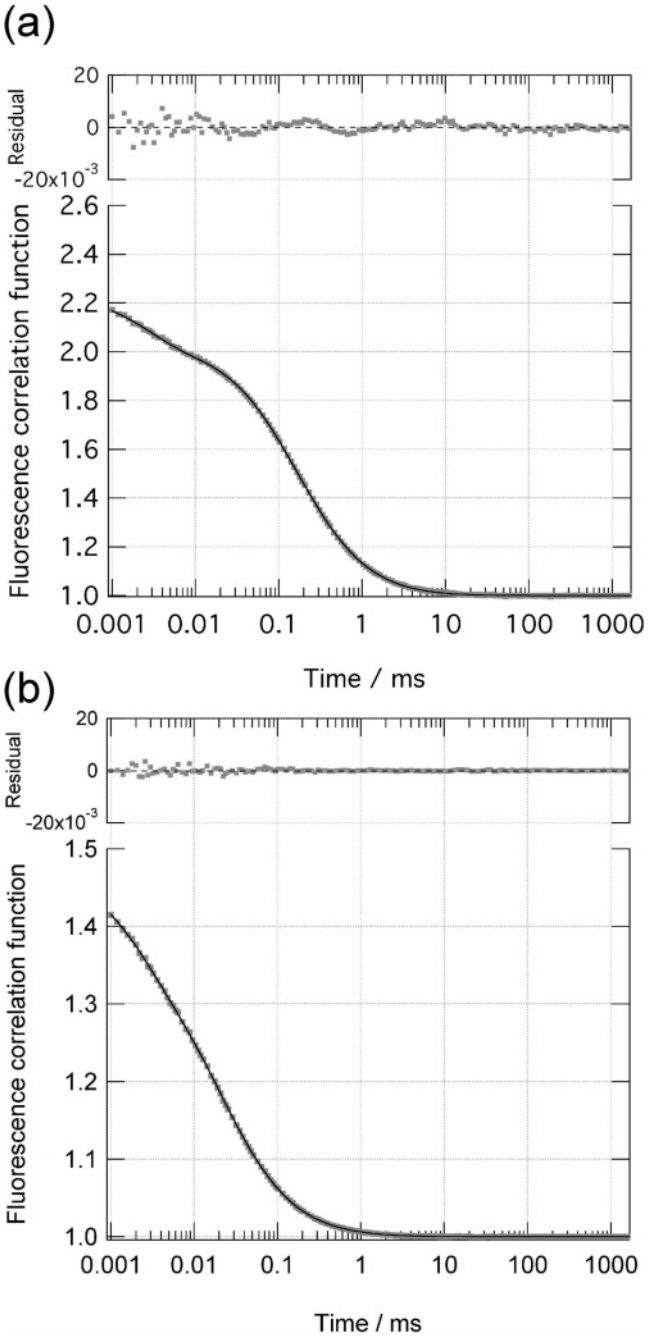

Figure 6. Typical fluorescence autocorrelation curves of the R6G in ethylene glycol (a) and R123 in water (b) with the NIR laser light at 240 mW, and their fitting curves based on eq 2 and residuals. Experimental data were plotted as gray dots and theoretical curves were drawn in a black solid line as in Figure 4. The theoretical model expressed by eq 2 well reproduces the autocorrelation curves even in the presence of the NIR laser irradiation.

with eq 4 and the temperature−viscosity relationships in Figure 2. This figure shows that the temperature at the focal point linearly increases with the incident NIR laser power in the region examined here. A similar linear relationship between the temperature and the incident NIR laser power was confirmed also for all other solutions used in the present work in the NIR power region up to 240 mW. The coefficient of the temperature rise versus the incident laser power was summarized in Table 1. No remarkable temperature elevation in D_2O solution again confirms the temperature elevation is due to the absorption of the NIR laser light by the solvents.

Discussion

As was shown in previous sections, the local temperature elevation, ΔT, in the solvents can be ascribed to the absorption of the 1064 nm laser beam and the difference of the temperature elevation coefficient among the solvent used was clearly observed (Figure 7). As is easily predicted, the $\Delta T/\Delta P$ value is closely related to the extinction coefficient, α, and the thermal conductivity of the solvents, λ. It can be considered that heat generated at the focal point of the trapping laser beam Q_{abs} is proportional to the extinction coefficient of the solvents, α, and the incident laser power, P.

$$Q_{abs} \propto \alpha P \tag{5}$$

To consider heat conduction from the focal spot of the NIR light, thermal conduction was assumed to take place from the small spherical heat source with a radius of r_1. This approximation leads to the one-dimensional heat conduction equation as represented by eq 6.

$$q = -\lambda \frac{dT}{dr} \tag{6}$$

Here, q is heat flux (W m^{-2}); λ is thermal conductivity (W m^{-1} K^{-1}); T is temperature (K); and r is the distance from the center of the spherical heat source. In the steady state, the heat generated in the small sphere, Q_{in}, is equal to the heat flow, Q_{flow}, from the sphere to the surroundings: $Q_{in} = Q_{flow} = 4\pi r^2 q$.

Substitution of eq 6 into this equation gives

$$\frac{dT}{dr} = -\frac{Q_{in}}{4\pi\lambda}\frac{1}{r^2} \tag{7}$$

Equation 7 is solved under the boundary condition $T = T_1$ at $r = r_1$, $T = T_{Room}$ at $r_2 = \infty$, and $Q_{in} = Q_{abs}$, then temperature change, ΔT, is given by the following

$$\Delta T \propto \frac{\alpha P}{\lambda}\left(\frac{1}{r_1}\right) \tag{8}$$

Then,

$$\Delta T/\Delta P \propto \frac{\alpha}{\lambda}\left(\frac{1}{r_1}\right) \tag{9}$$

Equation 8 predicts that the temperature at the focal point of the NIR light increases in proportion to the laser power P. This is confirmed experimentally for all solvents used here as already shown in Figure 7. Also the linear relationship between $\Delta T/\Delta P$ and α/λ predicted by eq 9 reproduced our experimental results as shown in the plot of $\Delta T/\Delta P$ as a function of α/λ in Figure 8. From these results, it can be concluded that the temperature elevation coefficient is qualitatively determined by these two parameters of solvents, α and λ.

As mentioned in the introductory section, the temperature elevation coefficients, $\Delta T/\Delta P$, of water were reported to be ~8 deg K/W by Schmidt et al.,[13] ~5 deg K/W by Fischer et al.,[9] 10−14.5 deg K/W by Tromberg et al.,[10,11] and ~19 deg K/W by Hell et al.[14] The present value of 22−24 deg K/W is a little higher than those previous experimental results and is comparable to the values by the elaborate calculation by Hell et al.

On the difference between the present value and those previously estimated by several experimental methods, it is worth noting that previous experimental approaches did not directly examine the temperature elevation in solvents induced

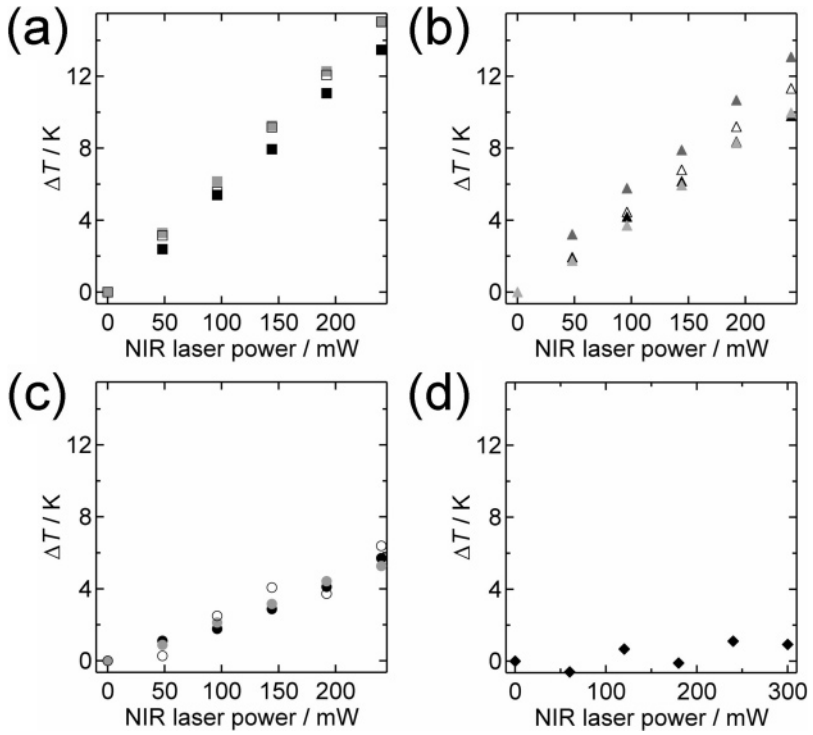

Figure 7. Temperature at the focal point of the NIR laser light estimated by the method proposed in the present report as a function of the incident laser power for the solution of ethylene glycol (a), ethanol (b), aqueous (c), and heavy water (d). The temperature elevation coefficients for these solutions are summarized in Table 1.

TABLE 1: Local Temperature Deviation, Extinction Coefficient, Thermal Conductivity, and Measuring Point (Distance between the Surface of the Sample Vessel and the Detection Point)

solvent	α [m^{-1}]	λ [W m^{-1} K^{-1}]	α/λ [W K^{-1}]	molecule	distance from the bottom of the sample cell [μm]	Δ*T*/Δ*P* [K/W] (exptl data)
ethylene glycol	19.9	0.26	75	R6G	30	56 ± 0.5
				R6G	30	63 ± 0.6
				R6G	30	64 ± 0.4
				R6G	20	66 ± 1
				R6G	5	67 ± 3
ethanol	11.2	0.17	69	R123	30	47 ± 0.5
				R6G	30	56 ± 0.9
				R123	30	42 ± 0.5
				R6G	30	42 ± 0.6
H_2O	14.5	0.59	24	R123	30	22 ± 0.8
				R123	30	24 ± 1.9
				R123	30	22 ± 0.3
D_2O	∼0		∼0	R6G	30	2.6 ± 0.1

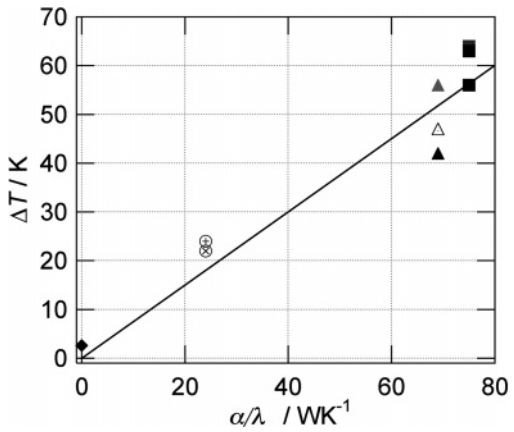

Figure 8. Plot of the temperature elevation coefficients, Δ*T*/Δ*P*, as a function of the ratio of the extinction coefficient of the solvents, α, to the thermal conductivity of the solvents, λ. The experimental values of Δ*T*/Δ*P* at 30 μm above the bottom of the sample cells in Table 1 are plotted by squares for ethylene glycol, by triangles for ethanol, by circles for water, and by a diamond for deuterated water.

by the irradiation of the NIR light. The phase transition with the latent heat and the heat capacity of the rather large beads may influence the temperature increase in the solvent. In contrast to these previous works, the present measurements provide more accurate information in determining the temperature elevation coefficient of solvent itself for the following reasons. First, we directly monitored the thermal motion of molecules inside the trapping potential well. Second, a small number of fluorescent molecules do not affect the temperature of the examined volume and thus the latent heat and the heat capacity of the probe system are not involved.

We will discuss the influence of glass substrate at the bottom of the sample cells. Local heating in the solvents used in the present experiment might be affected owing to the larger thermal conductivity of glass (typically ∼1.0 W m^{-1} K^{-1} at room temperature[22]) than that of the solvents. For experimentally elucidating the influence, we measured temperature in the ethylene glycol solution at several points from 5 to 30 μm from the surface of the sample chamber. The result, however, did not exhibit distance dependence between the surface of sample cells and measurement point as shown in Table 1. From these results, it can be concluded that the influence of glass substrate at the bottom does not seriously affect the temperature elevation at the focusing point of the NIR beam.

One may think about the gradient of temperature inside/around the focusing point of the NIR light. In the focal spot of the NIR light, the light intensity has the distribution expressed by Fraunhofer's diffraction theory. This intensity distribution might affect the estimation of temperature in the focal point of the trapping beam because the location of the sampling area in the FCS measurement varied from measurement to measurement within the spatial resolution of the optical microscope (∼200 nm). The experimental results of Δ*T*/Δ*P*, however, exhibited

good repeatability from measurement to measurement, indicating that the temperature did not have a steep gradient in the focal spot. The tight focusing of the intense laser beam for stable trapping also results in a steep gradient of the light intensity around the focal point, which might induce convection at the vicinity of the focusing area. In the present temperature estimation process, we neglected the effect of such convection because the autocorrelation functions of the sample solutions even under irradiation of the NIR light were well reproduced (as clearly shown in Figure 6) by the theoretical model of eq 1 that expresses fluorescence correlation signals under thermal equilibrium without convective flow. This indicates that the convection did not seriously affect the thermal motion of molecules in the sample solutions and then the effect was negligible in estimating local temperature through the present method.

Summary

In the present paper, we have proposed a method for measuring local temperature in solution using fluorescent correlation spectroscopy and applied it to elucidate local heating accompanying laser trapping. The local heating exhibited linear dependence on the NIR laser power. The temperature deviation of a few degrees K at the focus of the NIR laser light was measured: 56−63 deg K/W for ethylene glycol, 42−56 deg K/W for ethanol, and 22−24 deg K/W for water. These experimental results were qualitatively explained in view of the balance between the extinction coefficient and the thermal conductivity of the solvents.

In laser trapping experiments for micrometer-sized particles, typically a few tens of milliwatt laser power is introduced under an objective. In this case, temperature elevation could be as small as 2 K at the focus in aqueous solution. However, in the case of trapping nanometer-sized particles/polymers, much more laser power, a few hundreds of a milliwatt, is introduced to the focus, resulting in a temperature rise of a few to 10 deg K. This effect is not negligible in manipulating temperature-sensitive materials, such as proteins and some kinds of amphiphilic polymers exhibiting thermal phase transition.

It is worth noting that the present method permits temperature measurement in a very tiny area, ca. 350 nm without disturbance in the sample thanks to its high sensitivity and tiny amount of fluorescent probes of $\sim 10^{-9}$ M order. In contrast to the conventional methods, such as thermocouples and platinum sensors with higher heat capacity than the probe molecules used in our method, this feature is very significant especially in the application to temperature monitoring in a small amount of sample solution. We foresee our method will be useful for monitoring temperature in microfluidic systems, for measuring cell activities in terms of local temperature, and for elucidating dispersive structures closely related to temperature distribution in a small domain.

Acknowledgment. The present work was financially supported by The Mazda Foundation's Research Grant, The Iketani Science and Technology Foundation, the Ministry of Education, Culture, Sports, Science, and Technology (MEXT), Grant-in-Aid for Scientific Research on Priority Area "Molecular Nano Dynamics" and Grant-in-Aid for Young Scientists (B), and the 21st Century COE Program "Core Research and Advanced Education Center for Materials Science and Nano Engineering" from the Japan Society for the Promotion of Science (JSPS).

References and Notes

(1) Ashkin, A.; Dziedzic, J. M.; Bjorkholm, J. E.; Chu, S. *Opt. Lett.* **1986**, *11*, 288.
(2) Ito, S.; Yoshikawa, H.; Masuhara, H. *Appl. Phys. Lett.* **2001**, *78*, 2566.
(3) Ito, S.; Yoshikawa, H.; Masuhara, H. *Appl. Phys. Lett.* **2002**, *80*, 482.
(4) Ito, S.; Yoshikawa, H.; Masuhara, H. *Jpn. J. Appl. Phys.* **2004**, *43*, L885.
(5) Hofkens, J.; Hotta, J.; Sasaki, K.; Masuhara, H.; Iwai, K. *Langmuir* **1997**, *13*, 414.
(6) Hofkens, J.; Hotta, J.; Sasaki, K.; Masuhara, H.; Taniguchi, T.; Miyashita, T. *J. Am. Chem. Soc.* **1997**, *119*, 2741.
(7) Svoboda, K.; Schmidt, C. F.; Schnapp, B. J.; Block, S. M. *Nature* **1993**, *365*, 721.
(8) Kojima, H.; Muto, E.; Higuchi, H.; Yanagida, T. *Biophys. J.* **1997**, *73*, 2012.
(9) Wurlitzer, S.; Lautz, C.; Liley, M.; Duschl, C.; Fischer, M. *J. Phys. Chem. B* **2001**, *105*, 182.
(10) Liu, Y.; Cheng, D. K.; Sonek, G. J.; Berns, M. W.; Chapman, C. F.; Tromberg, B. J. *Biophys. J.* **1995**, *68*, 2137.
(11) Liu, Y.; Sonek, G. J.; Berns, M. W.; Tromberg, B. J. *Biophys. J.* **1996**, *71*, 2158.
(12) Celliers, P. M.; Conia, J. *Appl. Opt.* **2000**, *39*, 3396.
(13) Peterman, E. J. G.; Gittes, F.; Schmidt, C. F. *Biophys. J.* **2003**, *84*, 1308.
(14) Schönle, A.; Hell, S. W. *Opt. Lett.* **1998**, *23*, 325.
(15) Misawa, H.; Koshioka, M.; Sasaki, K.; Kitamura, N.; Masuhara, H. *J. Appl. Phys.* **1991**, *70*, 3829.
(16) *Fluorescence Correlation Spectroscopy;* Rigler, R., Elson, E. S., Eds.; Springer Series in Chemical Physics 65; Springer: Berlin, Germany, 2001.
(17) Krichevsky, O.; Bonnet, G. *Rep. Prog. Phys.* **2002**, *65*, 251.
(18) Riddick, J. A.; Bunger, W. B. *Organic Solvents*, 3rd ed.; Weissberger, A., Ed.; Techniques of Chemistry, Volume II; Wiley-Interscience: New York, 1970; pp 28−34.
(19) Magde, D.; Elson, E. L.; Webb, W. W. *Biopolymers* **1974**, *13*, 29.
(20) Dorn, I. T.; Neumaier, K. R.; Tampe, R. *J. Am. Chem. Soc.* **1998**, *120*, 2753.
(21) Masuda, A.; Ushdia, K.; Okamoto, T. *Biophys. J.* **2005**, *88*, 3584.
(22) *CRC Handbook of Chemistry and Physics*, 69th ed.; Weast, R. C., Astle, M. J., Beyer, W. H., Eds.; CRC Press: Boca Raton, FL, 1988; pp E7−E9.
(23) Hale, G. A.; Querry M. R. *Appl. Opt.* **1973**, *12*, 555.